

VENTRICULAR FUNCTION

The Angiotensin II Type 2 Receptor and Improved Adjacent Region Function Post-MI

CHRISTINA M. BOVE,¹ WESLEY D. GILSON,² CHRISTOPHER D. SCOTT,¹ FREDERICK H. EPSTEIN,^{2,3} ZEQUAN YANG,² JOSEPH M. DIMARIA,³ STUART S. BERR,³ BRENT A. FRENCH,² SANFORD P. BISHOP,⁴ and CHRISTOPHER M. KRAMER, M.D.,^{1,3,*}

¹Department of Medicine, University of Virginia Health System, Charlottesville, Virginia, USA

²Department of Biomedical Engineering, University of Virginia Health System, Charlottesville, Virginia, USA

³Department of Radiology, University of Virginia Health System, Charlottesville, Virginia, USA

⁴Department of Pathology, University of Alabama, Birmingham, Alabama, USA

Angiotensin II type 2 receptor (AT₂-R) overexpression in the mouse heart preserves left ventricular (LV) size and global LV function during post-MI remodeling. We hypothesized that CMR tagging would localize regional improvements in myocardial function during post-MI remodeling in AT₂-R cardiac overexpressed transgenic mice (TG), which could explain the preservation of global LV function post-MI. Six male wild-type (WT) C57BL/6 mice and 10 TG mice were studied by CMR at baseline (day 0) and days 1, 7, and 28 post-MI. MI was induced by 1 hour occlusion of the LAD followed by reperfusion. On day 1 post-MI, gadolinium-DTPA was injected to assess infarct size. LV size and function was assessed by cine CMR. Mean % circumferential shortening (%CS) was calculated within infarcted, adjacent, and remote regions at each time point in WT and TG mice. Quantitative interstitial collagen and mean myocyte cross-sectional area was measured postmortem at day 28 post-MI. LV end-systolic volume was lower and ejection fraction higher at baseline in the TG group and these differences were maintained post-MI. Within infarcted and remote zones, although %CS was higher in TG mice at day 0, there was no difference by day 28 between groups. Within adjacent regions, while there was no difference at day 0 or 1 in TG vs. WT, %CS was significantly higher in TG mice by day 7, and these changes persisted out to day 28 post-MI. Regional interstitial collagen and myocyte size were similar between groups. Thus, myocardial tagging can detect regional differences in contractile function post-MI in TG mice, and AT₂-R overexpression is associated with improved contractile function in adjacent noninfarcted myocardium.

Key Words: Angiotensin; Magnetic resonance imaging; Myocardial infarction; Remodeling; Receptors

1. Introduction

Most of the physiological effects of angiotensin II (AngII) are attributed to the angiotensin II type 1 receptor (AT₁-R) (1). The role of the angiotensin II type 2 receptor (AT₂-R) in left ventricular (LV) remodeling in disease states is an area of active investigation (2–6). In fact, many of the beneficial effects of AT₁-R blockade and angiotensin converting enzyme inhibition post-MI may be mediated by AngII stimulation of the AT₂-R (7, 8). We have previously shown that AT₂-R overexpression in the mouse heart preserves global LV size and function during post-MI remodeling (9).

In that study, the transgenic mice (TG) demonstrated preserved LV cavity size, wall thickness within the infarct zone, and global function during post-MI remodeling compared to wild-type controls (WT).

Myocardial tagged CMR studies have demonstrated regional heterogeneity of function in noninfarcted regions following acute MI (10). Regions remote from the infarct exhibit mildly reduced function early post-MI (11), while regions adjacent to the infarct demonstrate greater and persistent dysfunction (10, 12), in part related to myocyte hypertrophy and contractile dysfunction (13). Tagged CMR studies have been shown to be feasible in mouse models (14). Recently, our group has shown that these regional differences in contractile function exist in mice post-MI (15).

CMR tagging can therefore be used to measure regional improvements in myocardial function during post-MI remodeling in AT₂-R overexpressed mice. We hypothesized that improved adjacent zone function would help preserve global LV function post-MI previously shown in these transgenic mice and that some of the benefit would be

Received 19 April 2004; accepted 27 August 2004.

*Address correspondence to Christopher M. Kramer, M.D., Departments of Medicine and Radiology, University of Virginia Health System, Lee St., Box 800170, Charlottesville, VA 22908, USA; Fax: (434) 982-1618; E-mail: ckramer@virginia.edu

due to regional differences in interstitial collagen and/or myocyte hypertrophy.

2. Materials and methods

2.1. Animal model

Animal protocols were in accordance with the *Guide for the Care and Use of Laboratory Animals* (NIH publication No. 85-23, revised 1996) and were approved by the University of Virginia Animal Care and Use Committee. The transgenic mouse strain with cardiac overexpression of the AT₂-R on a C57BL/6 background was developed in the laboratory of H. Matsubara (16) as previously described (9, 17).

Six male wild-type (WT) C57BL/6 mice and 10 transgenic (TG) mice that overexpress the AT₂-R in the heart, aged 10–14 weeks, were studied by CMR at baseline (day 0) and days 1, 7, and 28 post-MI and were a subgroup of mice whose volumetric data was previously reported (18). MI was induced by a 1-hour occlusion of the LAD followed by reperfusion as previously described (9, 19). Noninvasive measurements of heart rate (HR) and systolic blood pressure (SBP) were performed at baseline and then weekly for the study duration using a Visitec-2000 tailcuff apparatus.

2.2. Mouse imaging

Anesthesia was induced with 3.0% inhaled isoflurane and maintained with 1.0% isoflurane administered with a nosecone during imaging. Imaging was performed on a Varian 200/400 Inova 4.7 T MRI system with Magnex gradients (80 G/cm maximum strength) and a custom-built Litz radio-frequency coil (Doty Scientific, Columbia, SC). On day 1 post-MI, 0.3 mM/kg gadolinium-DTPA (Gd) was infused intraperitoneally 20 minutes prior to imaging to assess infarct size. The ECG and core body temperature were monitored during imaging using an MR-compatible system for small animals (SA Instruments, Inc., Stony Brook, NY). Mouse body temperature was regulated to $37.0 \pm 0.1^\circ\text{C}$ during the imaging session with an external heating bath.

An ECG-triggered 2D cine FLASH sequence was used to obtain seven to eight 1-mm thick short-axis slices from apex to base. The echo time was (TE) = 3.9 ms, and TR was adjusted (8–10 ms) to obtain 16 phases per cardiac cycle. A 20° flip angle was used except on day 1 when a 60° flip angle was used to increase the amount of T1 weighting in post-contrast imaging. A 2.56×2.56 cm FOV was used with a matrix size of 128×128 . The tagging sequence used a double inversion recovery black blood SPAMM sequence as previously described (15) with a multiphase FLASH acquisition (Fig. 1). Specific parameters included: TR = 8–12 ms, TE = 5.5 ms, FOV = $2.56 \text{ cm} \times 2.56 \text{ cm}$, matrix size = 192 (readout) \times 96 (phase encode), slice thickness = 1 mm. The composite SPAMM flip angle was 180° and tag separation was 0.7 mm. Two sets of orthogonal tags were applied to each slice in separate acquisitions.

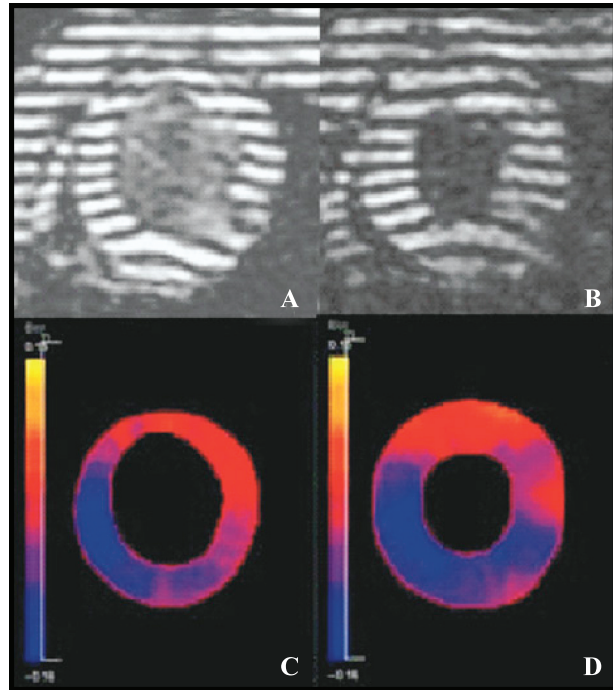


Figure 1. End-systolic tagged images (top panel A, B) and corresponding % circumferential shortening (CS) color maps (below C, D) on day 28 post-MI of a WT (left) and TG mouse (right). Blue color represents normal CS while red represents reduced CS. Notice the cavity dilation and wall thinning in the infarct zone in the WT mouse as compared to the TG mouse and more extensive dysfunction throughout the short axis.

2.3. Data analysis

Short-axis cine images were analyzed using ARGUS image analysis software (Siemens Medical Solutions, Princeton, NJ). Epi- and endocardial borders were planimetered to determine end-diastolic volume (EDV), end-systolic volume (ESV), left ventricular mass (LVM), and ejection fraction (EF). Volumes and mass were indexed to body weight (EDVI, ESVI, LVMI). The infarct region was defined as the area of delayed hyper-enhancement in day 1 post-Gd images with a signal intensity greater than two standard deviations above the mean of remote regions (Fig. 2) (20). Infarct size was measured from the contrast-enhanced cine images using ARGUS and calculated as percentage of total LV mass.

Percent circumferential shortening (%CS) was measured from tagged images using the Findtags program (21) (courtesy of M. Guttman, E. McVeigh, NIH) and 12 sectors per slice (Fig. 2). Epicardial and endocardial borders for tag analysis were traced. On day 1 images, two to three slices containing approximately 40–60% of the myocardial area with transmural contrast enhancement were subject to strain analysis. A 12-sector model was aligned such that the sector 1 border matched the Gd-enhanced border (Fig. 3). Sectors within the Gd-enhanced region were termed infarct, those bordering either side of the infarct in the short axis were termed adjacent, and all remaining sectors were termed

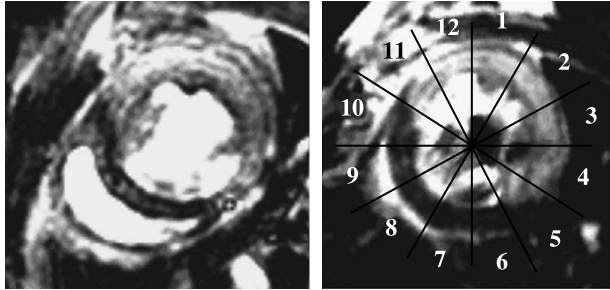


Figure 2. End-diastolic short axis gadolinium-enhanced MR images of a WT mouse (left) and TG mouse (right) on day 1 post-MI. The infarct region appears as the hyperenhanced area on each image, and is similar in size in both animals. In the image from the TG mice (right), the zone classification for tag analysis is superimposed. The analysis on day 1 post-MI is based on end-diastolic Gd-enhanced cine images. Infarcted segments are defined as the enhanced sectors 11 through 5 with one sector on either side of the infarct defined as adjacent (sectors 10 and 6). All remaining sectors (7–9) are defined as remote.

remote. For other time points (days 0, 7, and 28), corresponding slices were chosen for strain analysis with care taken to align the sectors in the same anatomical locations for each corresponding slice using papillary muscles and RV insertion sites as landmarks (Fig. 3). Mean %CS was calculated within each zone at each time point in WT and TG mice (Figs. 2 and 3).

2.4. Collagen analysis

After euthanasia, the heart was removed and fixed in formaldehyde. Fixed sections of myocardium were then embedded in paraffin, sectioned at 6 μm, and stained with

Table 1. Weekly noninvasive tail cuff systolic blood pressures in WT and TG mice (p = NS for all)

		Week 0	Week 1	Week 2	Week 3
BP (mmHg)	WT	104 ± 5	102 ± 5	109 ± 5	101 ± 11
	TG	109 ± 12	101 ± 7	112 ± 5	112 ± 5

picric acid sirius red. Quantitative morphometry was carried out on myocardium within 1.5 mm of the infarct border (adjacent) and more than 1.5 mm beyond the border (remote) in seven TG and six WT mice using an Olympus microscope with a green 540-nm filter and a CCD72 video camera interfaced to a computer with a Universal Imaging Image 1/AT morphometry system (West Chester, PA). A minimum of 35 fields approximately 575 × 750 μm each was measured from three or four sections from each region, and the volume % collagen calculated as the mean from all fields in each region for each animal.

2.5. Cell morphometry

Three to five tissues from adjacent and remote regions of each heart were sectioned at 5 microns thickness, stained with picric acid sirius red, and examined with an Olympus AH2 research microscope using rhodamine epifluorescence. Using a 40X objective (660X on monitor), cross-sectional area by region was determined on a minimum of 60 myocytes from the same seven TG and six WT animals, selected from areas judged to be within 20 degrees of true cross-section, using a Universal Imaging AT1 image analysis system (Universal Imaging, WestChester, PA), and mean area calculated for each animal and region.

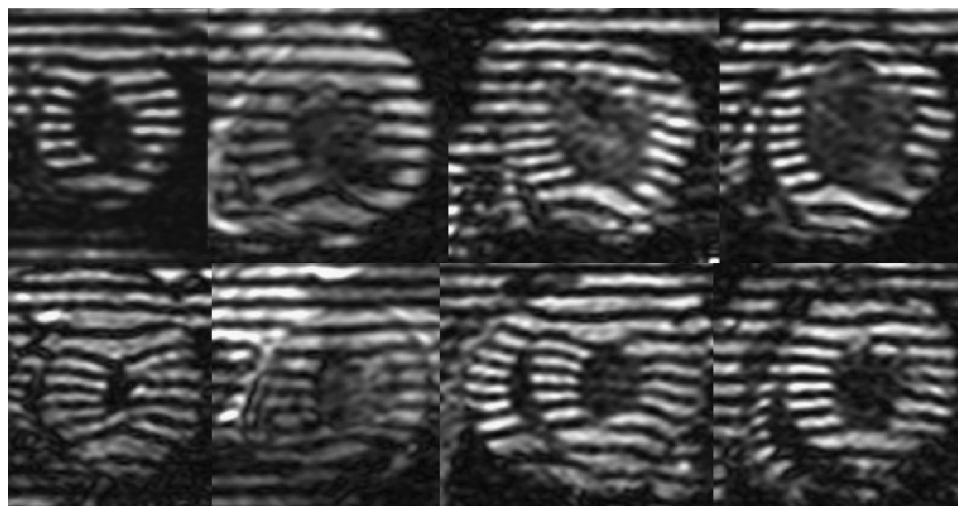


Figure 3. End-systolic short-axis tagged images in WT mice (top panel) and TG mice (bottom panel) at days 0, 1, 7, and 28 days post-MI from left to right. Greater cavity dilatation and more wall thinning in the infarct zone is seen in the WT mice, especially at days 7 and 28 post-MI.

Table 2. LV end-diastolic volume index, end-systolic volume index, mass index, and ejection fraction in WT and TG mice at each time point

	Strain	Baseline	Day 1	Day 7	Day 28
EDVI, $\mu\text{L/g}$	WT	1.75 ± 0.06	2.27 ± 0.09	3.16 ± 0.06	3.52 ± 0.13
	TG	1.50 ± 0.16	1.74 ± 0.10^a	2.36 ± 0.17^a	2.56 ± 0.23^a
ESVI, $\mu\text{L/g}$	WT	0.60 ± 0.06	1.35 ± 0.04	2.14 ± 0.09	2.33 ± 0.12
	TG	0.38 ± 0.23^a	0.73 ± 0.25^a	1.35 ± 0.53^a	1.41 ± 0.52^a
LVMI, mg/g	WT	2.55 ± 0.11	3.59 ± 0.12	3.72 ± 0.20	3.76 ± 0.11
	TG	3.14 ± 0.26	3.44 ± 0.28	3.72 ± 0.21	3.66 ± 0.25
EF, %	WT	66.4 ± 2.8	40.5 ± 1.5	32.3 ± 2.7	34.0 ± 2.4
	TG	75.8 ± 3.2^a	58.6 ± 3.7^a	44.1 ± 4.5	46.3 ± 3.4^a

^ap < 0.03 vs. WT.

2.6. Statistical analysis

Statistical analysis included two-way ANOVA to confirm intragroup differences by region and time point or group and time point. Infarct size for WT and TG mice was compared using paired Student's t-test. Regional (between-zone) and between-group differences in %CS were analyzed using pairwise multiple comparisons subtesting (Tukey test). Regional % collagen and cell size was compared between WT and TG mice by unpaired t-test and by region within a group by paired t-test. Data are presented as mean \pm SE.

3. Results

Weekly noninvasive tail cuff blood pressures were similar between groups (Table 1). Volumetric data are shown in Table 2 and are similar to those previously published, demonstrating smaller ESVI at each time point in TG including at baseline. EF was greater at baseline in TG, and parallel declines were seen in both groups. Mean % infarct size as % of LV mass was similar in both groups ($41.1 \pm 1.4\%$ in WT and $42.2 \pm 2.5\%$ in TG, p = NS) (Fig. 2).

In infarct segments, while there was higher %CS in TG mice compared to WT at day 0 ($14.8 \pm 0.3\%$ vs.

$12.0 \pm 0.4\%$ respectively, p < 0.001), %CS declined in both groups, and was similar by day 28 ($1.6 \pm 0.4\%$ for TG vs. $0.4 \pm 0.7\%$ for WT, p = 0.10) (Fig. 4). Similarly, for remote regions, although %CS was higher in TG at day 0 ($14.2 \pm 0.4\%$ vs. $12.0 \pm 0.6\%$, p = 0.004), by day 28 there was no difference ($12.6 \pm 0.5\%$ vs. $12.6 \pm 0.6\%$; TG vs. WT, p = NS) (Fig. 5). Within adjacent regions, %CS in TG and WT mice was similar at day 0, and fell in both groups beginning at day 1 post-MI and persisted to day 28 post-MI (Fig. 6). However, by day 7 post-MI, %CS was significantly higher in TG compared to WT ($10.3 \pm 0.7\%$ vs. $6.9 \pm 1.0\%$, respectively, p < 0.005), and these changes continued out to day 28 post-MI ($9.3 \pm 0.7\%$ vs. $5.9 \pm 1.0\%$, p < 0.004) (Fig. 6).

Mean interstitial collagen content in remote regions was similar between groups (Table 3). Collagen content was significantly higher in adjacent noninfarcted regions than remote regions in both groups, but not different between groups ($10.8 \pm 2.1\%$ in WT vs. $14.2 \pm 1.1\%$ in TG, p = NS) (Table 3). As a reference, mean % interstitial collagen in noninfarcted controls is $1.2 \pm 0.2\%$.

Mean cell cross-sectional area (CSA) in adjacent regions was similar between groups ($518 \pm 36 \mu^2$ in WT vs. $536 \pm 45 \mu^2$ in TG) (Table 3). Like collagen content, cell CSA was higher in adjacent than remote regions in both groups, but not

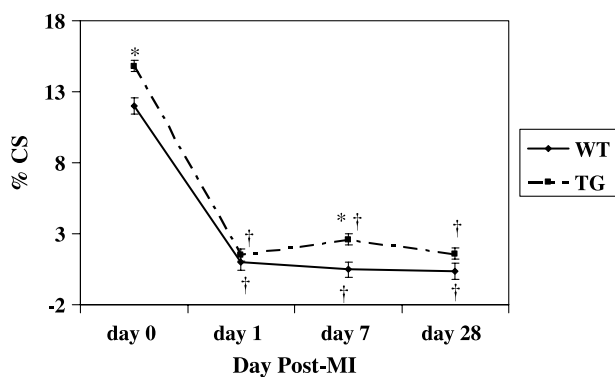


Figure 4. %CS in infarct regions from days 0–28 post-MI in WT and TG mice. *p < 0.005 vs. WT, †p < 0.001 vs. day 0.

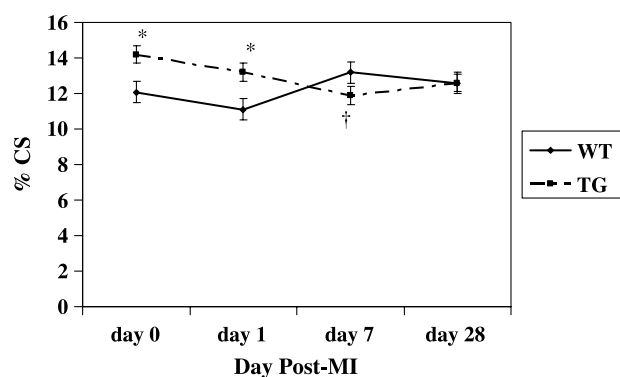


Figure 5. %CS in remote regions from days 0–28 post-MI in WT and TG mice. *p < 0.01 vs. WT, †p < 0.001 vs. day 0.

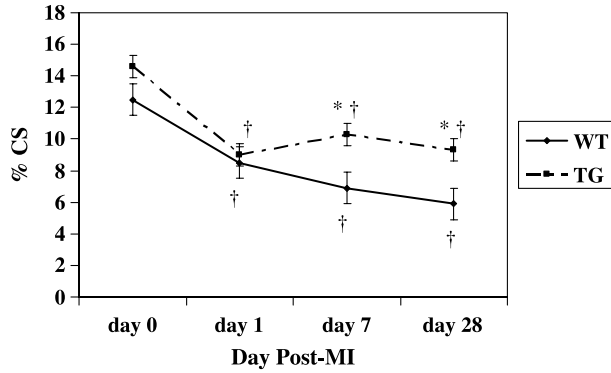


Figure 6. %CS in adjacent regions from days 0–28 post-MI in WT and TG mice. **p* < 0.005 vs. WT, †*p* < 0.03 vs. day 0.

different between groups (Table 3). As a reference, mean myocyte CSA in noninfarcted controls is 164 ± 31 μ².

4. Discussion

We have previously shown that myocardial tagging can be used to measure regional differences in contractile function post-MI in large animals (11) and humans (10). These findings have recently been extended to mice and allow the study of regional function in transgenic and knockout mice (15). The present study demonstrates the utility of MR tagging in the measurement of regional myocardial function in murine genetic models of disease.

AT₂-R overexpression in the murine heart is associated with improved global function at baseline compared to WT mice and preserved global systolic function during post-infarct LV remodeling (9). The volumetric data in the current study confirm our previously published findings. In the present study, we have shown that at baseline prior to MI, regional function is slightly better in TG than WT throughout the LV. In post-infarct TG mice, contractile function in adjacent noninfarcted myocardium at day 7 post-MI is superior to that of WT, and this difference persists to day 28 post-MI. No between-group differences in function within the infarct or remote noninfarcted regions were found. Thus, preserved adjacent region function accounts for the improved global LV function during post-MI remodeling seen with AT₂-R overexpression when compared to WT mice.

The mechanisms by which AT₂-R overexpression preserves systolic function post-MI are incompletely understood. Blood pressure was similar between groups during the study, suggesting that differences in afterload cannot explain these findings. Both regional interstitial collagen and myocyte size was similar between groups, which implies that neither differences in fibrosis or myocyte hypertrophy account for regional differences in function. This suggests that improved function in TG mice may be due to differences in myocyte function, although this was not directly measured in the

present study. Reduced preload may account for some of the benefit as in volumetric studies in these mice; LV end-diastolic volume index was smaller at days 7 and 28 post-MI time points in TG mice (9). However, if preload alone was the mechanism involved, improved function in both adjacent and remote regions might be expected.

Improved myocyte function in TG mice may be a mechanism for regional functional improvement. Controversy exists regarding the status of myocyte function in noninfarcted myocardium during LV remodeling. Previous studies have shown in a rat model of chronic MI that myocyte function in noninfarcted regions is normal (22, 23). We have shown in an ovine model that isolated adjacent noninfarcted myocytes are dysfunctional relative to remote noninfarcted myocytes that function normally (13). At 8 weeks post-MI in this model, myocyte % contraction was decreased in adjacent regions (6.4 ± 0.4%), as compared with remote (8.8 ± 0.5%, *p* < 0.01), and was associated with decreased amplitude of Ca⁺⁺ transients and L-type Ca⁺⁺ current density (13). This regional heterogeneity of function in noninfarcted regions may be difficult to demonstrate *ex vivo* in isolated myocytes in small animal models, but can be demonstrated *in vivo* using MR tagging as in the present study.

Bradykinin and nitric oxide (NO) pathways have been shown to be important in downstream signaling of the AT₂-R in vascular smooth muscle (24). The same pathways may apply to myocardial AT₂-R signaling. A specific AT₂-R agonist, CPG 42112, increased eNOS expression in myocytes by 2.4-fold (25). eNOS expression was increased by direct AngII stimulation and antagonized by an AT₂-R antagonist PD 123319. *In vivo*, in AT₂-R knockout mice, eNOS protein expression was significantly reduced (25). These studies suggest that AngII stimulation of the AT₂-R is responsible for increases in eNOS and resultant beneficial cardiac effects. Studies by our group in the same model have shown that treatment with the nitric oxide synthase inhibitor L-NAME from day 1 through 28 post-MI allows remodeling to progress unchecked in TG mice with AT₂-R overexpression (18).

Table 3. Regional interstitial collagen and myocyte cross-sectional area in WT and TG mice

	WT	TG	<i>p</i>
Adjacent % interstitial collagen	10.8 ± 2.1	14.2 ± 1.1	NS
Remote % interstitial collagen	1.2 ± 0.4	1.5 ± 0.3	NS
<i>p</i>	< 0.01	< 0.01	
Adjacent myocyte cross-sectional area	518 ± 36 μ ²	536 ± 45 μ ²	NS
Remote myocyte cross-sectional area	287 ± 23 μ ²	332 ± 36 μ ²	NS
<i>p</i>	< 0.02	< 0.02	

5. Limitations

Isolated myocyte function was not examined in the present study and may have enabled insight into mechanisms of improved regional function in TG mice. The heart was not fixed at a particular point in the cardiac cycle postmortem, which may affect assessment of myocyte size. Delayed contrast enhanced imaging for infarct localization was done only at day 1 post-MI. Newer pulse sequence designs are presently in development to enable this imaging to take place at later time points post-MI for matching with tagged images. Due to time considerations with post-infarct mice in the scanner, the entire heart was not covered with short-axis myocardial tagging. However, the density of data acquired with tagging allows precise measurement and localization of regional myocardial function. Matching of slices from the day 1 study to later time points is a potential problem, but care was taken to landmark the slices based on RV insertion sites, papillary muscles, and apex-to-base location.

Acknowledgments

This work was supported by RO1 HL-52980 (CMK), AHA Mid-Atlantic Affiliate Grant-in-Aid 0256343U (CMK), and T32 HL07355 (CMB).

References

- Matsubara H. Pathophysiological role of angiotensin II type 2 receptor in cardiovascular and renal diseases. *Circ Res* 1998; 83:1182–1191.
- Ichihara S, Senbomatsu T, Price E Jr, Ichiki T, Gaffney FA, Inagami T. Angiotensin II type 2 receptor is essential for left ventricular hypertrophy and cardiac fibrosis in chronic angiotensin II-induced hypertension. *Circulation* 2001; 104:346–351.
- Inagami T, Senbonmatsu T. Dual effects of angiotensin II type 2 receptor on cardiovascular hypertrophy. *Trends Cardiovasc Med* 2001; 11:324–328.
- Oishi Y, Ozono R, Yano Y, Teranishi Y, Akishita M, Horiuchi M, Oshima T, Matsubara H. Cardioprotective role of AT₂ receptor in postinfarction left ventricular remodeling. *Hypertension* 2003; 41:814–818.
- Schneider MD, Lorell BH. AT(2) judgment day: which angiotensin receptor is the culprit in cardiac hypertrophy? *Circulation* 2001; 104:247–248.
- Opie LH, Sack MN. Enhanced angiotensin II activity in heart failure: reevaluation of the counterregulatory hypothesis of receptor subtypes. *Circ Res* 2001; 88:654–658.
- Xu J, Carretero OA, Liu YH, Shesely E, Yang F, Kapke A, Xang XP. Role of AT₂ receptors in the cardioprotective effect of AT₁ antagonists in mice. *Hypertension* 2002; 40:244–250.
- Liu Y-H, Yang X-P, Sharov VG, Nass O, Shabbah HN, Peterson E, Carretero OA. Effects of angiotensin-converting enzyme inhibitors and angiotensin II type 1 receptor antagonists in rats with heart failure. *J Clin Invest* 1997; 99:1935.
- Yang Z, Bove CM, French BA, Epstein FH, Berr SS, Dimaria JM, Gibson J, Carey RM, Kramer CM. Angiotensin II type 2 receptor overexpression attenuates post-infarction left ventricular remodeling. *Circulation* 2002; 106:106–111.
- Kramer CM, Lima JA. C, Reichek N, Ferrari VA, Palmon LC, Yeh I-T, Tallant B, Axel L. Regional function within noninfarcted myocardium during left ventricular remodeling. *Circulation* 1993; 88:1279–1288.
- Kramer CM, Rogers WJ, Theobald TM, Power TP, Petruolo S, Reichek N. Remote noninfarcted region dysfunction soon after first anterior myocardial infarction: a magnetic resonance tagging study. *Circulation* 1996; 94:660–666.
- Melillo G, Lima JAC, Judd RM, Goldschmidt-Clermont PJ, Silverman HS. Intrinsic myocyte dysfunction and tyrosine kinase pathway activation underlie the impaired wall thickening of adjacent regions during postinfarct left ventricular remodeling. *Circulation* 1996; 93:1447–1458.
- Kim Y-K, Kim S-J, Kramer CM, Yatani A, Tagaki G, Mankad S, Singh D, Szigeti GP, Bishop SP, Shannon RP, Vatner DE, Vatner SF. Altered excitation-contraction coupling in myocytes from remodeled myocardium after chronic myocardial infarction. *J Mol Cell Cardiol* 2002; 34:63–73.
- Zhou R, Pickup S, Glickson SD, Scott CH, Ferrari VA. Assessment of global and regional myocardial function in the mouse using cine and tagged MRI. *Magn Reson Med* 2003; 49:764.
- Epstein FH, Yang Z, Gilson WD, Berr SS, Kramer CM, French B. MR tagging after myocardial infarction in mice demonstrates contractile dysfunction in adjacent and remote noninfarcted regions. *Magn Reson Med* 2002; 48:399–403.
- Masaki H, Kurihara T, Yamaki A, Inomata N, Nozawa Y, Mori Y, Murasawa S, Kizima K, Maruyama K, Horiuchi M, Dzau VJ, Takahashi H, Iwasaka T, Inada M, Matsubara H. Cardiac-specific overexpression of angiotensin II AT₂ receptor causes attenuated response to AT₁ receptor-mediated pressor and chronotropic effects. *J Clin Invest* 1998; 101:527–535.
- Kurisu S, Ozono R, Oshima T, Kambe M, Ishida T, Sugino H, Matsuura H, Chayama K, Teranishi Y, Iba O, Amano K, Matsubara H. Cardiac angiotensin II type 2 receptor activates the kinin/NO system and inhibits fibrosis. *Hypertension* 2003; 41:99–107.
- Bove CM, Yang Z, Gilson WD, Epstein FH, French B, Berr SS, Bishop SP, Matsubara H, Carey RM, Kramer CM. Nitric oxide mediates benefits of angiotensin II type 2 receptor in post-infarct remodeling. *Hypertension* 2004; 43:680–685.
- Yang Z, Zingarelli B, Szabo C. The crucial role of endogenous interleukin-10 production in myocardial ischemia-reperfusion injury. *Circulation* 2001; 101:1019–1026.
- Yang Z, Berr SS, Gilson WD, Toufektsian MC, French BA. Simultaneous evaluation of infarct size and cardiac function in intact mice by contrast-enhanced cardiac magnetic resonance imaging reveals contractile dysfunction in noninfarcted regions early after myocardial infarction. *Circulation* 2004; 109:1161–1167.
- Guttman MA, Prince JL, McVeigh ER. Tag and contour detection in tagged MR images of the left ventricle. *IEEE Trans Med Imag* 1994; 13:74–88.
- Anand IS, Liu D, Chugh SS, Prahash AJ, Gupta S, John R, Popescu F, Chandrashekar Y. Isolated myocyte contractile function is normal in postinfarct remodeled rat heart with systolic dysfunction. *Circulation* 1997; 96:3974–3984.
- Gupta S, Prahash AJ, Anand IS. Myocyte contractile function is intact in the post-infarct remodeled rat heart despite molecular alterations. *Cardiovasc Res* 2000; 48:77–88.
- Tsutsumi Y, Matsubara H, Masaki H, Kurihara H, Murasawa S, Takai S, Miyazaki M, Nozawa Y, Ozono R, Nakagawa K, Miwa T, Kawada N, Mori Y, Shibasaki Y, Tanaka Y, Fujiyama S, Koyama Y, Fujiyama A, Takahashi H, Iwasaka T. Angiotensin II type 2 receptor overexpression activates the vascular kinin system and causes vasodilatation. *J Clin Invest* 1999; 104:925–935.
- Ritter O, Schuh K, Brede M, Rothlein N, Burkard N, Hein L, Neyses L. AT₂ receptor activation regulates myocardial eNOS expression via the calcineurin-NF-AT pathway. *Faseb J* 2003; 17:283–285.